Quantifying lens elastic properties with optical coherence elastography as a function of intraocular pressure

Chen Wu[a], Hongqiu Zhang[a], Manmohan Singh[a], Salavat R. Aglyamov[b,c], and Kirill V. Larin[a,d,e*]

[a]Department of Biomedical Engineering, University of Houston, Houston, TX
[b]Department of Mechanical Engineering, University of Houston, Houston, TX
[c]Department of Biomedical Engineering, University of Texas at Austin, Austin, TX
[d]Interdisciplinary Laboratory of Biophotonics, Tomsk State University, Tomsk, Russia
[e]Molecular Physiology and Biophysics, Baylor College of Medicine, Houston, TX

[*]Corresponding author: klarin@uh.edu

ABSTRACT

Normal intraocular pressure (IOP) is crucial for proper maintaining of eye-globe geometry, ocular tissue health, and visual acuity. An elevated IOP is associated with diseases such as glaucoma and uveitis. While the effects of an elevated IOP on the delicate tissues of the optic nerve head and retina are well-studied, the changes in lenticular biomechanical properties as a function of IOP are not as clear. Moreover, changes in lenticular biomechanical properties have been implicated in conditions and diseases such as presbyopia and cataract. However, measuring the biomechanical properties of the lens as it sits inside the eye-globe is a challenge, but it is necessary to correctly understand the interplay between lenticular biomechanical properties and IOP. In this work, we utilized optical coherence elastography (OCE) to measure the biomechanical properties of the porcine lens *in situ*.

Keywords: Optical coherence elastography (OCE), intraocular pressure (IOP), lenticular biomechanical properties, crystalline lens

1. INTRODUCTION

A healthy intraocular pressure (IOP) is crucial to maintaining normal eye-globe geometry [1-3], and many ocular diseases, such as glaucoma and uveitis, are correlated with elevated IOP. The sclera and cornea will endure large stresses at high IOPs, which can cause diseases, such as myopia and keratoconus [4]. However, it is difficult to investigate the biomechanical properties of the crystalline lens *in situ* or *in vivo* due to its location inside the eye-globe, and much of previous research has been focused on utilizing the "gold standard" of mechanical testing on extracted lenses [5, 6]. Mechanical testing, however, is invasive and does not replicate the true lenticular environment in the eye-globe. Nevertheless, previous research has shown an increase in the stiffness of the lens as a function of age [7, 8]. Thus, measuring changes in lenticular biomechanical properties may provide earlier detection of lenticular certain pathologies, such as cataract. Ultrasound elastography (USE) [1, 9]and magnetic resonance elastography (MRE) [10] are clinically-established elastographic imaging techniques, but their need for contact-based excitation, relatively poor spatial resolution, and low contrast may not be suitable for lenticular applications. In this work, we utilized a noninvasive optical coherence elastography (OCE) technique to assess lens biomechanical properties, which has sub-nanometer levels of displacement sensitivity with phase-resolved detection [11-13].

In this study, we investigated the changes in the biomechanical properties of porcine lenses as a function of IOP using a co-aligned acoustic radiation force (ARF) and phase-sensitive optical coherence tomography (OCT) system. The OCE measurements were performed with the eye-globe intact, and the IOP was increased from 10 to 40 mmHg

Optical Elastography and Tissue Biomechanics VI, edited by Kirill V. Larin, Giuliano Scarcelli, Proc. of SPIE
Vol. 10880, 108801P · © 2019 SPIE · CCC code: 1605-7422/19/$18 · doi: 10.1117/12.2510225

at 5 mmHg step. The ARF remotely induced small amplitude (<10 μm) localized displacements at the apex of the porcine lens, which then propagated as an elastic wave. The elastic wave group velocity was used to qualitatively assess the stiffness change of the crystalline lens while cycling IOP. The results demonstrated that the stiffness of the crystalline lens increases along with IOP.

2. MATERIALS AND METHODS

The schematic of the experimental setup is shown in Figure 1. The phase-sensitive OCE system consisted of a spectral domain optical coherence tomography (SD-OCT) and ARF delivery systems. The SD-OCT system was based on a superluminescent light diode (SLD) with a central wavelength of 840 nm, bandwidth of 49 nm, and output power of 18 mW. The acquisition speed of line scan camera was set to 25 kHz. Acoustic radiation force induced low amplitude displacements (<10 μm) at the apex of the lenses. The elastic wave propagation was detected by the OCE system, which had a displacement sensitivity of ~7 nm in air. Whole porcine eye-globes (N=3) were cannulated with two needles for IOP control. One needle was connected via tubing to a saline-filled syringe placed in a micro-infusion pump. The other needle was connected via tubing to the pressure transducer [14]. A Matlab (MathWorks, Natick, MA) GUI program was developed to control the closed-loop artificial IOP control system. The IOP was controlled by infusion or extraction of saline from the syringe.

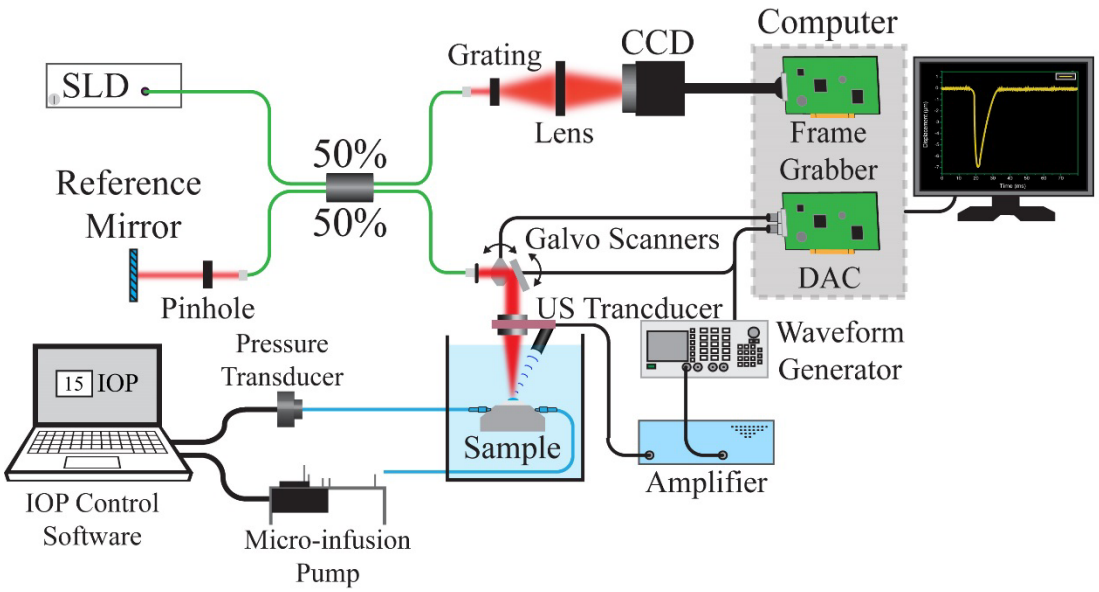

Figure 1. Schematic of the OCE experimental setup. CCD – charged coupled device; DAC – digital to analog converter.

The OCE measurements were made at IOPs of 10 mmHg to 40 mmHg with 5 mmHg increments, which covers a normal and elevated IOP range [2]. Successive M-mode images ($n = 251$) were acquired over a ~6.1 mm line, where the center of the scan and ARF excitation were at the apex of the lens. The group velocity of the elastic wave was determined by the slope of a linear fit of the wave propagation distances and the corresponding propagation times [15]. The Young's modulus, E, was estimated by the surface wave equation, $E = \frac{2\rho(1+\nu)^3}{(0.87+1.12\nu)^2} c_g^2$, where ρ=1.183g/L was the density [16], ν=0.5 was Poisson's ratio [7], and c_g was the OCE-measured elastic wave group velocity.

3. RESULTS AND DISCUSSION

Figure 2 plots the change in group velocity and Young's modulus as estimated by the surface wave equation for each of the samples, when IOP increases. The group velocity and the stiffness of the lenses increased along with IOP, and this trend was observed in all samples. This effect of stiffening is the result of lens deformation and consequent exhibition of the nonlinear elastic properties of the lens. Such result is in agreement with our previous results, where

ultrasound shear wave elastography and model-based OCE were used [1, 17]. However, the stiffening of the lens as a function of IOP has been shown to be less pronounced than in the cornea in our previous works [1, 18]. A possible explanation of this difference is that the lens undergoes less deformation during IOP elevation than cornea, such that the nonlinear elastic properties of the lens do not play as significant role in response to the external simulation as compared to the cornea.

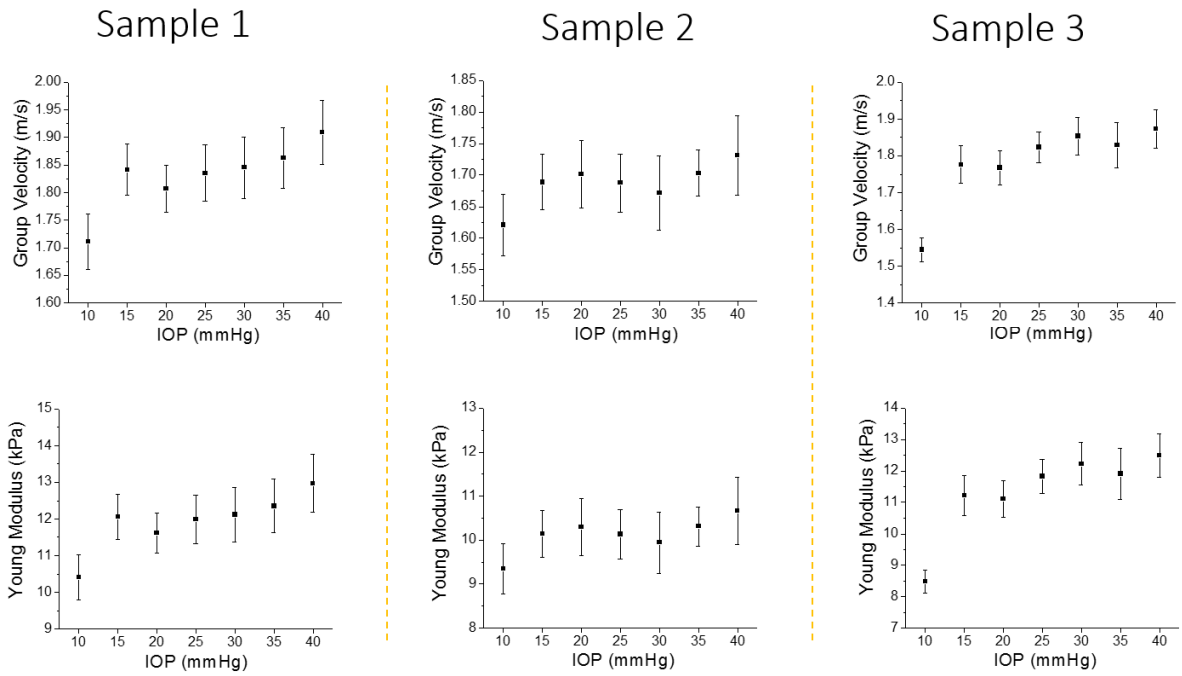

Figure 2. The group velocity and the estimated Young's moduli of three samples. The top row illustrates the group velocity, and the bottom row shows the Young's modulus as estimated by the surface wave equation.

Figure 3 shows that the average group velocity and the Young's modulus of the lenses increased from 9.5 ± 0.9 kPa at 10 mmHg IOP to 12.2 ± 0.8 kPa at 40 mmHg. There is also a noticeable plateau when the IOP increased beyond 15 mmHg IOP. After 15 mmHg IOP, the Young's modulus of the lens increased at a much smaller rate as a function of IOP.

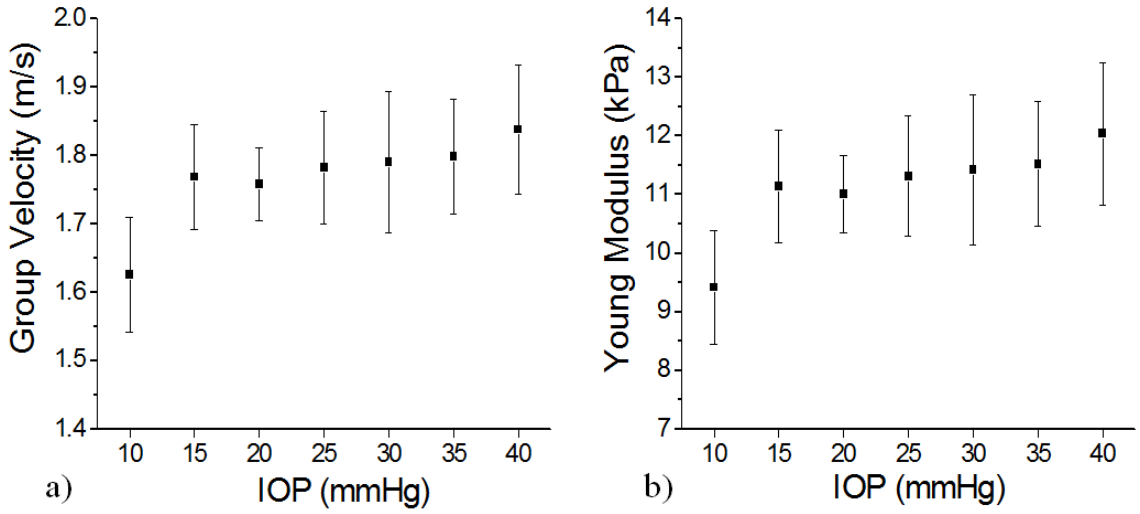

Figure 3. a) The average group velocity and b) the estimated Young's moduli for all of the samples.

Further work is required to develop more robust analytical wave models that can quantify the lens biomechanical properties accurately by incorporating the true lens geometry and boundary conditions. Additionally, the lenticular nonlinear elastic properties must be considered for accurate biomechanical characterization to understand the non-monotonic increase in lenticular stiffness as a function of IOP.

4. CONCLUSIONS AND FUTURE WORK

In this study, we evaluated the changes of *in situ* porcine lenticular biomechanical properties while increasing the eye-globe intraocular pressure. The results show that the lens stiffness increased but appeared to plateau at higher IOPs (> 15 mmHg). OCE can assess lenticular biomechanical properties and may be useful for detecting and, potentially, characterizing the risk of the threats of the lens which harm its stiffness. Our future work will entail utilizing a more robust mechanical wave model to obtain quantitative biomechanical parameters such as viscoelasticity.

5. ACKNOWLEDGEMENTS

This work was supported by grant R01EY022362 from the National Institute of Health, Bethesda, MD, USA

REFERENCES

[1] S. Park, H. Yoon, K. V. Larin *et al.*, "The impact of intraocular pressure on elastic wave velocity estimates in the crystalline lens," Phys Med Biol, 62(3), N45-N57 (2016).

[2] I. Grierson, and W. R. Lee, "The fine structure of the trabecular meshwork at graded levels of intraocular pressure:(1) Pressure effects within the near-physiological range (8–30 mmHg)," Experimental eye research, 20(6), 505-521 (1975).

[3] K. Mercieca, D. Perumal, K. Darcy *et al.*, "Cataract extraction after deep sclerectomy and its effect on intraocular pressure control," Eye, 1 (2018).

[4] A. Böhm, M. Kohlhaas, R. Lerche *et al.*, "Measuring intraocular pressure in keratoconus. Effect of the changed biomechanics," Der Ophthalmologe: Zeitschrift der Deutschen Ophthalmologischen Gesellschaft, 94(11), 771-774 (1997).

[5] H. A. Weeber, G. Eckert, F. Soergel *et al.*, "Dynamic mechanical properties of human lenses," Exp Eye Res, 80(3), 425-34 (2005).

[6] S. Krag, and T. T. Andreassen, "Biomechanical measurements of the porcine lens capsule," Exp Eye Res, 62(3), 253-260 (1996).
[7] R. F. Fisher, "The elastic constants of the human lens," J Physiol, 212(1), 147-80 (1971).
[8] K. R. Heys, S. L. Cram, and R. J. Truscott, "Massive increase in the stiffness of the human lens nucleus with age: the basis for presbyopia?," Mol Vis, 10, 956-63 (2004).
[9] K. W. Hollman, M. O'donnell, and T. N. Erpelding, "Mapping elasticity in human lenses using bubble-based acoustic radiation force," Experimental eye research, 85(6), 890-893 (2007).
[10] D. V. Litwiller, S. J. Lee, A. Kolipaka *et al.*, "MR elastography of the ex vivo bovine globe," Journal of Magnetic Resonance Imaging, 32(1), 44-51 (2010).
[11] J. Schmitt, "OCT elastography: imaging microscopic deformation and strain of tissue," Opt Express, 3(6), 199-211 (1998).
[12] K. V. Larin, and D. D. Sampson, "Optical coherence elastography - OCT at work in tissue biomechanics [Invited]," Biomed Opt Express, 8(2), 1172-1202 (2017).
[13] M. Sticker, C. K. Hitzenberger, R. Leitgeb *et al.*, "Quantitative differential phase measurement and imaging in transparent and turbid media by optical coherence tomography," Opt Lett, 26(8), 518-20 (2001).
[14] M. D. Twa, J. Li, S. Vantipalli *et al.*, "Spatial characterization of corneal biomechanical properties with optical coherence elastography after UV cross-linking," Biomed Opt Express, 5(5), 1419-27 (2014).
[15] S. Wang, A. L. Lopez, 3rd, Y. Morikawa *et al.*, "Noncontact quantitative biomechanical characterization of cardiac muscle using shear wave imaging optical coherence tomography," Biomed Opt Express, 5(7), 1980-92 (2014).
[16] A. S. Vilupuru, and A. Glasser, "Optical and biometric relationships of the isolated pig crystalline lens," Ophthalmic Physiol Opt, 21(4), 296-311 (2001).
[17] C. Wu, S. R. Aglyamov, Z. L. Han *et al.*, "Assessing the biomechanical properties of the porcine crystalline lens as a function of intraocular pressure with optical coherence elastography," Biomedical Optics Express, 9(12), 6455-66 (2018).
[18] M. Singh, J. Li, Z. Han *et al.*, "Investigating elastic anisotropy of the porcine cornea as a function of intraocular pressure with optical coherence elastography," Journal of Refractive Surgery, 32(8), 562-567 (2016).